Enhanced imaging of SAGD steam chambers using broadband electromagnetic surveying

Sarah G. R. Devriese and Douglas W. Oldenburg, Geophysical Inversion Facility, University of British Columbia*

SUMMARY

In this paper, we propose using electromagnetic (EM) methods to monitor the growth of a SAGD steam chamber in an oil sands reservoir. In the past, 2D crosswell DC resistivity survey data have been acquired and interpreted with some success. We show that two-dimensional inversions of crosswell DC data produce low quality images with artifacts. The images are improved by carrying out 3D inversions. However, much improvement can be obtained by using full band EM surveys in either the frequency- or time-domain. Practical implementation of EM highly depends on the survey design. Here, we advocate a simple approach based on galvanic and magnetic responses of compact bodies. This provides a good starting point for any field survey and can be refined as geology becomes more complex. The major impact of our work is that with broadband EM and a limited number of transmitters and receivers, it is possible to obtain substantially better images compared to traditional crosswell DC resistivity. The results provide optimism for using 3D EM for time-lapse imaging of SAGD steam chambers.

INTRODUCTION

The Athabasca oil sands in Northern Alberta are one of the largest oil reserves in the world (Humphries, 2008). However, 80% of the oil sands are too deep for mining and require in-situ extraction methods, such as Steam Assisted Gravity Drainage (SAGD). In SAGD, two horizontal wells are drilled at the bottom of the bitumen reservoir. Steam is injected into the top well and a steam chamber grows upwards and outwards (Figure 1). The steam heats the oil which drains downwards and is captured by the second well. The success of this technique is dependent upon having the steam propagate throughout the bitumen reservoir. Unfortunately, mudstone laminations in the reservoir can prevent the steam from propagating as desired. It is therefore important to monitor the growth of the steam chambers (Charles et al., 2013). Currently, this is done with 4D seismic methods, which has proven to be successful in many cases. However, it may be limited by low sensitivity in the petro-elastic parameters to changes in fluid content, saturation, and porosity. A more complete interpretation of the extent of the steam chamber can be made if a method which is sensitive to changes in the pore-fluid is included.

Electrical conductivity is significantly affected by the injection of steam into a heavy oil reservoir (Mansure et al., 1993). EM methods therefore have potential to image steam chambers (Engelmark, 2010) but the methodologies have not been rigorously tested. Usually, electrical resistivity tomography (ERT) is acquired in vertical wells, as done by Tøndel et al. (2013) for SAGD in a pilot study program. Other applications of ERT for fluid-monitoring are discussed in the literature (e.g. Ramirez et al. (1993)). However, the combination of less-than-optimal survey design and potential restriction to 2D inversions yields lower quality images that may be contaminated by artifacts.

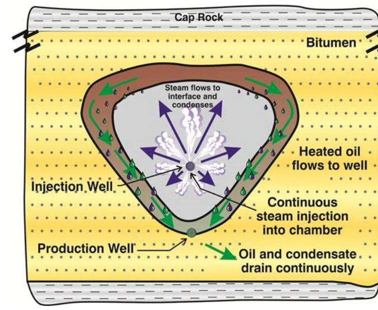

Figure 1: In SAGD, two horizontal wells are drilled near the bottom of the reservoir. The top injects steam into the reservoir, from which a chamber grows upwards and outwards. The steam heats the bitumen, which becomes fluid and flow downwards to the production well. The condensed steam is also produced. Figure courtesy of Suncor.

By expanding to frequency-domain EM, the earth is sampled differently at each frequency, and hence, joint inversion of many frequencies can provide higher resolution than working with DC data alone. The same holds for time-domain EM. Our work investigates how EM can provide greater information about time-lapse SAGD steam chambers. In order to monitor the chamber growth, the background conductivity (before steam is injected) must be recovered using a combination of EM surveys and borehole logging information. This baseline model can then be used as a reference model when inverting for the steam chambers at several time steps to monitor the growth. Such inversions requires a second, localized survey that focuses on the steam chamber. Any survey requires both the specification of the transmitter and receivers types and locations. In EM, there are ample choices: grounded (as in traditional DC resistivity) or inductive (an ungrounded wire loop) transmitters which can be on the surface or in boreholes, and receivers can measure voltages and/or 3-components of the magnetic field. In this paper, we introduce an equivalent problem that simplifies the EM physics to determine transmitter locations for a localized EM survey that detects and recovers a small chamber.

SYNTHETIC RESISTIVITY MODEL

We build a representative resistivity model by using the main units in the Athabasca oil sands. A synthetic, irregular steam chamber is generated by translating a snapshot of a 4D seismic attribute map into height (Figure 2). A subset of the data is used to create a synthetic steam chamber (Figure 3). The 10 Ωm pyramid-shaped anomalous steam body varies in thickness from 5 m to 50 m. It extends 150 m in the easting direction

DOI http://dx.doi.org/10.1190/segam2014-1247.1

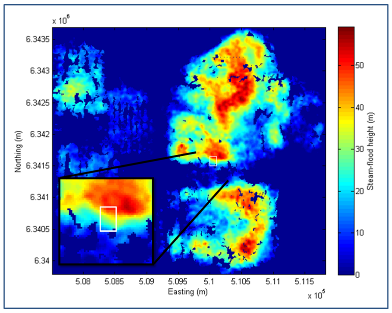

Figure 2: Seismic attribute data was used to simulate irregular steam chambers. The color of this image shows the height (in m) of steam chambers across multiple SAGD pads. The white rectangle is the subset of this field model utilized to represent a synthetic, but realistic, small steam anomaly.

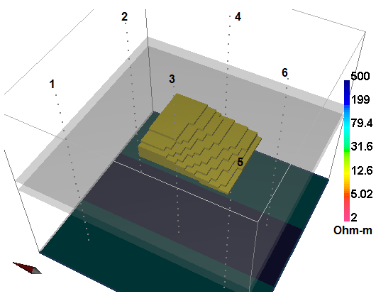

Figure 3: Oblique view of the pyramid-shaped synthetic resistivity model used in this paper. The confined steam anomaly (10 Ωm) underlies a conductive cap rock (17 Ωm). The top and bottom of the cap rock are shown as 2 gray surfaces. The anomaly and cap rock are hosted in a 400 Ωm background. Note that the cap rock and the steam anomaly are not in contact. The gray dots represent the electrode locations in the six vertical wells.

and 200 m in the northing direction. The 50 m-thick bitumen layer extends from $z = -200$ m to $z = -250$ m. Overlying the bitumen is a 25 m-thick conductive cap rock from $z = -175$ to $z = -200$ m with a resistivity of 17 Ωm. The cap rock is an important element in the model since it attenuates fields that propagate through it and channels currents away from the steam flood. The steam anomaly and the cap rock are hosted in a 400 Ωm background.

DIPOLE MOMENT-BASED SURVEY DESIGN

Two criteria must be satisfied in order for a survey to provide useful data: (a) the EM fields from a transmitter must have sufficient strength and orientation to couple with the sought body and generate significant anomalous currents; and (b) receivers must be close enough and have the correct orientation to detect the anomalous EM fields in the presence of various types of noise. Both of these items can be addressed, at least to first order, by working with a simplified resistivity model and approximating the excitation using galvanic and magnetic dipoles.

To do so, the conductivity of the earth σ can be decomposed into $\sigma = \sigma_0 + \Delta\sigma$ where σ_0 is a background conductivity and $\Delta\sigma$ is the conductivity of the anomalous body. The background conductivity can be simple, such as a uniform or layered earth in which the solution can be derived (semi-)analytically, or it may be more complicated and require numerical modeling. The EM fields from any conductivity are found by solving the quasi-static Maxwell's equations. In the frequency-domain, these are:

$$\nabla \times \mathbf{E} + i\omega\mu\mathbf{H} = 0, \tag{1}$$

$$\nabla \times \mathbf{H} - \sigma\mathbf{E} = \mathbf{J}_e, \tag{2}$$

where $\mathbf{J}_s$ is the source current density. Here, $\mathbf{E}$ is the electric field and $\mathbf{H}$ is the magnetic field. The fields are related to the fluxes by the constitutive relations $\mathbf{J} = \sigma\mathbf{E}$ and $\mathbf{B} = \mu\mathbf{H}$. The electrical conductivity σ relates the current density $\mathbf{J}$ and the electric field while the magnetic permeability μ relates the magnetic field to the magnetic flux density $\mathbf{B}$. Here, we assume the earth's magnetic permeability is constant, so $\mu = \mu_o$, where μ_o is the permeability of free space. The electrical resistivity is $\rho = 1/\sigma$, and is interchangeably used in place of conductivity.

Using the electric field, we calculate the anomalous current density $\mathbf{J}_a$ within the anomalous body:

$$\mathbf{J}_a = \Delta\sigma\mathbf{E}. \tag{3}$$

Next, we compute representative galvanic and inductive dipole moments. The galvanic dipole moment $\mathbf{m}_g$ points in the same direction as the anomalous electric currents while the inductive dipole moment $\mathbf{m}_i$ depends upon the cross-product of the anomalous currents with their positions:

$$\mathbf{m}_g = \int_v \mathbf{J}_a(\mathbf{r}')dv' \approx \sum_{k=1}^{K} \mathbf{J}_{ak}\Delta v_k, \tag{4}$$

$$\mathbf{m}_i = \frac{1}{2}\int_v \mathbf{r} \times \mathbf{J}_a(\mathbf{r}')dv' \approx \frac{1}{2}\sum_{k=1}^{K} \mathbf{r}_k \times \mathbf{J}_{ak}\Delta v_k. \tag{5}$$

K is the number of cells that comprise the anomalous body, Δv_k is the volume of each cell, and $\mathbf{r}$ is the distance between the anomalous current vector location $\mathbf{r}'$ and the centroid location $\mathbf{r}^c$: $\mathbf{r} = \mathbf{r}' - \mathbf{r}^c$. The centroid of the anomalous currents is analogous to the center of mass of a body and its location is written as:

$$\mathbf{r}^c = \frac{\int_v \mathbf{r}'|\mathbf{J}_a(\mathbf{r}')|dv}{\int_v |\mathbf{J}_a(\mathbf{r}')|dv} \approx \frac{\sum_{k=1}^{K} \mathbf{r}'_k|\mathbf{J}_{ak}|\Delta v_k}{\sum_{k=1}^{K} |\mathbf{J}_{ak}|\Delta v_k}. \tag{6}$$

A stronger dipole moment means the excitation in the anomalous body is greater: this yields larger secondary fields. Therefore, the strength of the dipole moment can be used as a proxy for the level of excitation in the anomalous body due to a given transmitter. Ideally, we want to excite the body from as many directions as possible, thus we also consider the azimuthal and elevation angles of the moments.

DOI http://dx.doi.org/10.1190/segam2014-1247.1

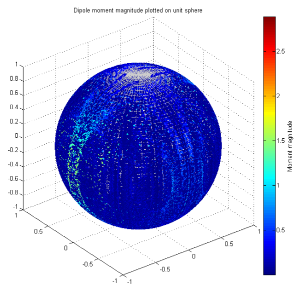

Figure 4: The galvanic moments from approximately 170,000 transmitters are plotted on a unit sphere, indicating that nearly every excitation direction is represented. Colorbar indicates dipole magnitude.

Selection of the transmitters is demonstrated with an example using galvanic borehole transmitters. We approximate the steam in Figure 3 by a 25 m radius sphere and surround it by 61 possible vertical observation wells. The wells extend from the surface to 400 m in depth and are spread out equally across a 1000 m by 1500 m area. Each well is populated with electrodes, spaced every 20 m in depth to provide sufficient data coverage. The total 1281 electrodes generate 1.6 million galvanic transmitter combinations. We impose a distance restriction between the electrodes so they can be in separate but nearby wells, reducing the possible transmitters to approximately 170,000. For each transmitter, we analytically calculate the primary electrostatic field in a halfspace of 400 Ωm. The response of a 10 Ωm anomalous sphere in the presence of the primary electrostatic field provides the anomalous current density (Ward and Hohmann, 1988). Subsequently, the galvanic dipole moment is calculated using Equation 4, where Δv is the volume of the sphere. In the presence of an electrostatic field, there is no inductive dipole moment.

The galvanic moments are plotted on a unit sphere (Figure 4), which is divided into n regions of equal area (Leopardi, 2006), where n is the number of desired transmitters; in this example, $n = 24$. From each region, we choose the transmitter that generates the largest moment. The final transmitters thus have large dipole strengths and a good sampling of directions, allowing each chosen transmitter to uniquely excite the anomalous body. Figure 5(a) shows the distribution of the 24 selected transmitters. We note that the selected transmitters lie close to the anomalous body because large dipole moment magnitudes were favored. This supports the distance restriction imposed: a large distance between current electrodes would give a weak dipole moment and would not be selected using our approach anyway.

The survey design approach easily translates to time-domain EM or inductive source EM with the use of numerical forward modeled anomalous currents. Depending upon the transmitter geometry however, not all regions of the unit sphere will be sampled (i.e. as when using current loops at the surface) because the moment directions are limited. In our example, excitation occurred in many directions because borehole transmitters were used. To address the influence of the cap rock, we compared the analytically-calculated moments to those calculated numerically for a model that includes the cap rock. To first order, the moments are similar, so we use the analytically-derived survey to compute EM data based on the model in Figure 3. Using numerical modeling, we can easily use the design method for geologically-complex models.

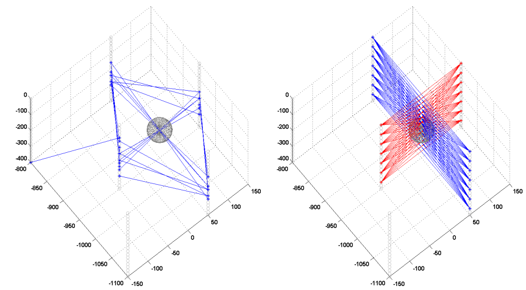

(a) (b)

Figure 5: The dipole moment-based survey (a) and two typical 2D ERT crosswell surveys (b). The gray dots represent the receiver electrodes in each of the six wells. The current electrodes for each transmitter are connected by a line for visibility. The sphere, representing the steam chamber, is also shown.

By default, secondary EM fields will be largest close to the anomalous body. Due to limitations of borehole placement, receivers are placed in the wells containing the transmitters, ensuring the closest position to the anomalous body. This provides 124 receivers per transmitter.

We compare the EM data to a traditional ERT survey with 4 times more transmitters (Figure 5(b)), as might be typically used in industry. The ERT geometry consists of two 2D crosswell DC resistivity surveys, providing 98 transmitters and 40 voltage measurements per transmitter. In the next section, we invert the data from both the dipole moment-based EM survey and the ERT survey.

2D AND 3D ERT INVERSIONS

Using the synthetic model in Figure 3, DC resistivity data were computed in 3D on an octree mesh (Haber et al., 2012). Oldenburg and Li (2005) provide an overview of the principles of forward modeling and inversion of geophysical data. Once forward modeled, we assign uncertainties as a percentage of the data with a noise floor. Here, we used 10% of the data plus a 0.004 V noise floor. These uncertainties are kept consistent for every DC inversion, whether 2D or 3D. For each inversion, the reference model contains the 17 Ωm cap rock in a 400 Ωm background. We first invert the two ERT surveys separately in 2D (Oldenburg and Li, 1994). However, for this survey geometry, the inverse models are plagued with artifacts and do not adequately recover the anomaly.

To combat these issues, the data from the two ERT surveys were simultaneously inverted in 3D (Haber et al., 2012). The recovered model shows drastic improvement: the anomaly is

DOI http://dx.doi.org/10.1190/segam2014-1247.1

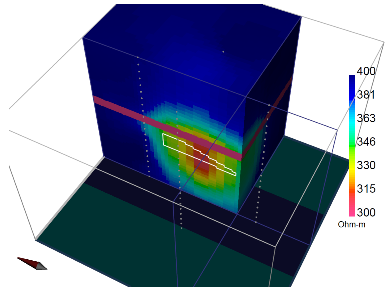

Figure 6: The 2D ERT data is inverted in 3D. The recovered anomaly is smooth and spherical in shape and is much more resistive than the true model. Note that the cap rock has a resistivity of 17 Ωm but is clipped on this color scale to better show the recovered anomaly. The gray dots represent the electrode locations in the four vertical wells used for this survey.

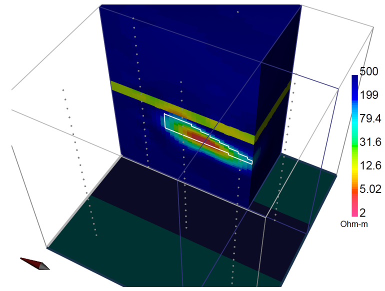

Figure 7: The electromagnetic data is inverted in 3D. The true anomaly is outlined in white. The pyramid-shape of the true anomaly is nicely recovered and the resistivity approaches the true value. The recovered anomaly is clearly distinguished from the cap rock. The gray dots represent the electrode locations in the six vertical wells.

confined between the wells and no artifacts are present (Figure 6). These results show that it is critical to invert the data in 3D, even if the survey is only oriented in 2 dimensions, because a 2D inversion cannot properly fit data due to a 3D anomaly. We also note that combining the two ERT surveys provides a better model than if each survey was inverted separately. Thus, transmitters in 3D orientations are critical to obtain adequate information about the shape and location of the anomaly. However, the lack of resolution in the 3D DC resistivity inversion motivates us towards EM methods, where different frequencies can provide more information.

FREQUENCY-DOMAIN 3D EM INVERSION

Using the 24-transmitter survey generated with the dipole moment approach, we forward model EM data at 7 frequencies ranging from 1 Hz to 10 kHz on an octree mesh in 3D. Uncertainties of 10% plus a floor were assigned to the data. The uncertainty floor was 10^{-5} V/m for the electric field and 10^{-6} A/m for the magnetic field. The inversion used the z-component of the electrical field and the 3 components of the magnetic field. The initial and reference model contained the 17 Ωm cap rock in a background of 400 Ωm. All model cells were active, meaning that the inversion can alter the cap rock and background model cells. Figure 7 shows the recovered resistivity model. The anomalous steam is well-recovered and distinctly separated from the cap rock. Although smooth, the shape of the recovered anomaly mimics the pyramid-shape of the true model. The anomaly's resistivity is near the true value but is overestimated in the center. The recovered resistivity of the cap rock is slightly altered, but overall remains close to the true model value. This result signifies that the geophysical method and the survey design are sensitive to the anomalous body, and the inversion is able to recover the anomaly adequately, even in the presence of a highly conductive cap rock layer.

When comparing the 3D EM inversion (Figure 7) to the 3D inversion of the ERT data (Figure 6), the EM model is clearly superior. Inversion of the EM data recovers the anomalous steam body, both in shape and resistivity, whereas the DC resistivity model has much lower resolution and accuracy. This highlights the superiority of electromagnetic data and the dipole moment-based survey design compared to traditional ERT surveys.

CONCLUSIONS

This work demonstrates the effectiveness of electromagnetic methods over traditional 2D ERT for imaging SAGD steam chambers in the Athabasca oil sands. The research is on-going: currently, we are investigating time-domain systems where the use of full waveform EM can provide more information about the steam chamber. Inductive sources are also being considered, especially from the surface as the primary magnetic field may penetrate the conductive cap rock and thus excite the underlying steam chamber. This would significantly decrease costs compared to borehole sources. By researching these options, our work aims to increase understanding of how EM can be utilized to monitor SAGD chambers over time and develop time-lapse inversion approaches to recover steam chamber growth. Additionally, the approaches we develop carry over to other time-lapse exploration topics, such as groundwater flow or tracking of contamination plumes.

ACKNOWLEDGMENTS

We would like to thank Sylvestre Charles and Suncor for their involvement in this research and their permission to present the seismic data.

DOI http://dx.doi.org/10.1190/segam2014-1247.1

http://dx.doi.org/10.1190/segam2014-1247.1

EDITED REFERENCES

Note: This reference list is a copy-edited version of the reference list submitted by the author. Reference lists for the 2014 SEG Technical Program Expanded Abstracts have been copy edited so that references provided with the online metadata for each paper will achieve a high degree of linking to cited sources that appear on the Web.

REFERENCES

Charles, S., J. Hostetler, J. Lin, and X. Luo, 2013, Squeezing every last drop out of a coarse 3D oil sands dataset for refining 3D survey design — A case history: Presented at the GeoConvention Integration.

Engelmark, F., 2010, Heavy oils: Reservoir characterization and production monitoring: SEG, 301–308.

Haber, E., J. Granek, D. Marchant, E. Holtham, D. Oldenburg, and R. Shekhtman, 2012, 3D inversion of DC/IP data using adaptive OcTree meshes: Presented at the 82nd Annual International Meeting, SEG.

Humphries, M., 2008, North American oil sands: History of development, prospects for future: Technical Report, Congressional Research Service.

Leopardi, P., 2006, A partition of the unit sphere into regions of equal area and small diameter: Electronic Transactions on Numerical Analysis, **25**, 309–328.

Mansure, A. J., R. F. Meldau, and H. V. Weyland, 1993, Field examples of electrical resistivity changes during steamflooding: SPE Formation Evaluation, **8**, no. 1, 57–64, http://dx.doi.org/10.2118/20539-PA.

Oldenburg, D. W., and Y. Li, 1994, Inversion of induced polarization data: Geophysics, **59**, 1327–1341, http://dx.doi.org/10.1190/1.1443692.

Oldenburg, D. W., and Y. Li, 2005, Near-surface geophysics: SEG, 59–150.

Ramirez, A., W. Daily, D. LaBrecque, E. Owen, and D. Chesnut, 1993, Monitoring an underground steam injection process using electrical resistance tomography: Water Resources Research, **29**, no. 1, 73–87, http://dx.doi.org/10.1029/92WR01608.

Tøndel, R., S. Dümmong, H. Schütt, A. Ducrocq, R. Godfrey, J. Ingham, and D. Labrecque, 2013, Reservoir monitoring in oil sands using a permanent cross-well system — Status and results after 18 months of production: Presented at the 75th Annual International Conference and Exhibition, EAGE.

Ward, S. H., and G. W. Hohmann, 1988, Electromagnetic methods in applied geophysics: SEG, 131–311.